Journal of Labelled Compounds and Radiopharmaceuticals

Published online 13 May 2010 in Wiley Interscience (www.interscience.wiley.com) DOI: 10.1002/jlcr.1768

10th International Symposium on the Synthesis and Applications of Isotopes and Isotopically Labelled Compounds—New Analytical Methods

Session 8, Wednesday, June 17, 2009

SESSION CHAIRS: DEAN CLODFELTER[a] AND ANTHONY REES[b]

[a]Eli Lilly, USA
[b]GE Healthcare, UK

Abstract: Different methods for the analysis of radiolabelled compounds are discussed as well as their potential uses in a wide range of activities such as drug discovery and ultra low level background LSC in a salt mine.

Keywords: accelerator mass spectrometry; microdosing; optogalvanic spectroscopy; ultra-low level scintillation counting; radiosynthesis; microfluidics

SOMETHING OLD, SOMETHING NEW–APPLICATIONS OF ACCELERATOR MASS SPECTROMETRY IN TRANSLATIONAL MEDICINE

R COLIN GARNER

Xceleron Ltd, The Biocentre, Innovation Way, York YO10 5NY, United Kingdom and Hull York Medical School, University of York, York, YO10 5DD, United Kingdom

Abstract: The enabling technology of accelerator mass spectrometry (AMS) permits ultrasensitive analysis of ^{14}C in the attogram to zeptogram range. As a result AMS analysis is being used in drug development to measure drug concentrations from human clinical studies conducted with very low amounts (nanoCuries) of administered radiolabel. The administered radiolabel can be at high specific radioactivity as in Phase 0 microdose studies or at much lower specific radioactivity as in metabolite profiling/mass balance and absolute bioavailability studies. Each of these study designs can give essential human ADME/PK information enabling drugs to be developed more effectively than using conventional approaches.

Keywords: accelerator mass spectrometry; microdosing; ADME/PK; absolute bioavailability

Introduction: Developing new drugs for the treatment of life threatening diseases is a costly and time consuming process. Bringing a new drug to market can take anywhere between 12–15 years and cost upwards of $1 billion.[1] Research productivity by the pharmaceutical and biotechnology industries has been falling year on year even though R&D expenditures have exponentially increased.[2] Indeed there were fewer new drug marketing approvals by the regulatory authorities last year than there were in the mid-90's. It has been estimated that the current R&D annual expenditure by the pharmaceutical industry is approximately $75 billion worldwide. Many of the blockbuster drugs are coming off patent and growth in revenues of some of the world's largest pharmaceutical companies have fallen back to historically low levels.[3,4] Despite this crisis, large pharmaceutical companies still appear to be slow in adopting new approaches despite the US FDA encouraging innovation through it's Critical Path initiative.[5]

The main reasons for this collective failure are the high attrition rate of novel molecules as they progress through the development path. Drugs fail for three major reasons–lack of clinical efficacy, adverse patient events and preclinical toxicology. These can comprise up to 80% of drug failures; considerable efforts are being made to identify new approaches that can avert these problems.[6,7] The causes of drug failure are multifarious but one major cause is inappropriate pharmacokinetics. Human ADME and PK properties will determine what makes a molecule 'druggable'.[8] Poor absorption, high clearance, large volumes of distribution, etc all can contribute to a molecule with potentially good pharmacology never making it as a marketable drug.

A good understanding therefore of human PK, as early as possible in the drug development process, is highly desirable since the development of molecules with poor PK characteristics can be terminated before too much expenditure has been incurred in their development. A number of novel methods have been introduced to predict human PK including *in vitro* studies using human

recombinant P-450's, *in silico* PB/PK modelling and tissue engineered human liver. However there is no better model for humans than humans. Putting this adage into reality requires new sensitive analytical procedures such as accelerator mass spectrometry (AMS), positron emission tomography (PET) and ultrasensitive mass spectrometry.

Today allometric scaling methods are used routinely by the pharmaceutical industry to predict human PK. Allometry uses a combination of *in vitro* and preclinical models to predict drug clearance. Allometry is an empirical approach which computes body mass and surface area between model species to predict human metabolism. There is always a degree of uncertainty in such predictions, leading to the possible further development of a molecule that when eventually tested in humans has inappropriate PK characteristics. The value of the AMS technology is in permitting earlier human PK studies, so that poorly metabolised drugs can be discarded before large resources are expended on their development.

The AMS technology: Developed over 40 years ago[8,9], AMS is a nuclear physics technique that counts individual atoms of elemental isotopes. At the heart of the instrument is a tandem Van der Graaff generator producing the necessary voltage to energise the atoms under investigation so that they can be counted atom by atom. New AMS instruments have been developed which are more compact than the original AMS instrumentation and which are particularly suitable for biomedical use.[9,10] These smaller instruments use a high voltage power supply to ionise the atoms rather than a tandem accelerator. Although the ionised species differs with the smaller accelerators, they appear to be of almost equal precision and accuracy to the large instruments. Certainly for biomedical AMS, the small instruments are quite adequate.

The most utility of the AMS technology for biomedical research is in the analysis of the three isotopes of carbon–^{12}C, ^{13}C and ^{14}C. The latter has a natural abundance of 1 part per trillion or 10^{-12} $^{14}C/^{12}C$ and hence makes it an attractive isotope to study. A small increase (10%) above the background is highly significant. AMS has exquisite sensitivity to measure ^{14}C when this isotope is used to label drugs, intermediary metabolic pathways or macromolecules.[11–13] AMS can analyse ^{14}C in the attogram to zeptogram range (10^{-18} to 10^{-21} g range).

The use of AMS in drug development was pioneered by the University of York, UK spinout company Xceleron. The demonstration of the power of AMS has encouraged one major pharmaceutical company to set up its own AMS centre.

AMS use in human ADME/PK translational medicine studies: The study of the metabolic disposition and fate of ^{14}C-labelled drugs in animals and humans has been undertaken since the discovery of ^{14}C and the ability to measure this isotope by decay counting methods in the early 1950's. AMS has permitted the routine analysis of ^{14}C in drug development at amounts which are several orders of magnitude lower than using conventional decay counting methods. For example a typical human radioactive dose for an AMS study is 200 nanoCurie (7 kBq) whilst for a conventional decay counting study, a dose of 100 microCuries (3.5 MBq) is normally administered. The AMS dose can be administered at high specific radioactivity which is the case for a Phase 0 microdose study or diluted with cold drug to administer at a pharmacological dose; the latter is termed a light label study.[14,15]

(i) Human Phase 0 microdose studies

First proposed in 1999 as a means of screening drug candidates for human ADME/PK properties[16], human Phase 0 microdose studies are becoming increasingly used in the following scenarios;

- Where animal models and/or *in vitro* metabolism studies give variable results making prediction of human PK difficult
- Where animal models and/or *in vitro* metabolism studies give similar human PK predictions for a series of candidate molecules making it difficult to select which molecule to take forward
- To help select the first dose for a conventional Phase I study
- To validate animal models for pharmacology and toxicology
- To determine the likely cost of goods

When the concept of microdosing was introduced there was considerable debate as to whether or not dose proportionality was seen between a microdose and a pharmacological dose. This matter is now resolved in that over twenty molecules have been examined at a microdose and a pharmacological dose. Linear PK is found in the majority of cases. In Table 1 are listed a number of development drugs as to their stage in development and the predictivity of the microdose/pharmacological dose comparison. It is interesting to note that for real development molecules as opposed to those used in the CREAM trial and EUMAPP, that a 100% correspondence was found.

The fact that a ^{14}C labelled drug is required for AMS analysis means that each molecule to be studied needs to be ^{14}C labelled in contrast to analysis using LC/MS. On the other hand provided the labelling is in a metabolically stable position, full quantitation of the parent drug and all its metabolites is possible without the need for internal deuterated standards.

(ii) Metabolite profiling and mass balance studies

As drugs are progressed down the development path, more and more metabolism information is required to meet regulatory needs. The US FDA published in early 2008, its latest guidance document[17] in which it requests drug developers to investigate metabolic

Table 1. Number of NCEs in development which have been dosed at a microdose and a pharmacological dose (source–Xceleron Ltd)

	No of NCEs by development stage
Phase I	4
Phase II/III	5
Marketed	1
Linear PK	**10 out of 10**

pathways for their drugs are early as possible. The FDA require both qualitative and quantitative PK information so that a comparison can be made between human metabolism and that in the animal species used for safety testing. The Agency have seen in some drug submissions an inappropriate test species used causing lengthy development delays. How pharma companies respond to the guidance document is still under discussion. For example, the Agency request that all metabolites comprising 10% or greater of parent drug at steady state conditions be characterised and it be demonstrated that the safety testing species produces the same spectrum of metabolites. This is a burdensome request if LC/MS is used as the routine analytical method but is relatively straightforward if AMS is used.

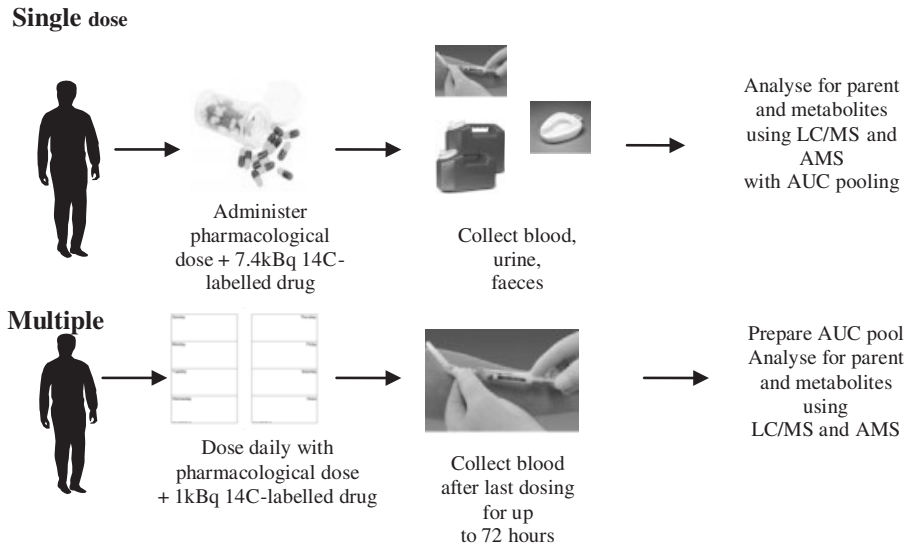

Figure 1. Study designs for mass balance/metabolite profiling studies.

A typical study design for a metabolite profile/mass balance study is shown in Figure 1. Using a small quantity of ^{14}C-labelled drug in a pharmacological dose background (a) obviates the requirement to conduct radiation dosimetry studies as the radioactive dose is so small as to be insignificant compared to background radiation and (b) allows the study to be built into Phase I protocols either by 'piggy-backing' onto a study arm or setting up a small satellite group.

Once blood and excreta samples are collected from study subjects in this study design, samples can either be fully analysed for parent drug and metabolites or a very simple AUC pool approach can be taken. In the latter approach, varying volumes of plasma are pooled according to the study length either within subjects or across subjects and the pooled sample is analysed by AMS after HPLC separation of a plasma extract. The relative peak heights obtained between metabolites and parent will reflect the relative proportion of the metabolites versus parent drug. An example of the approach is shown in Figure 2.

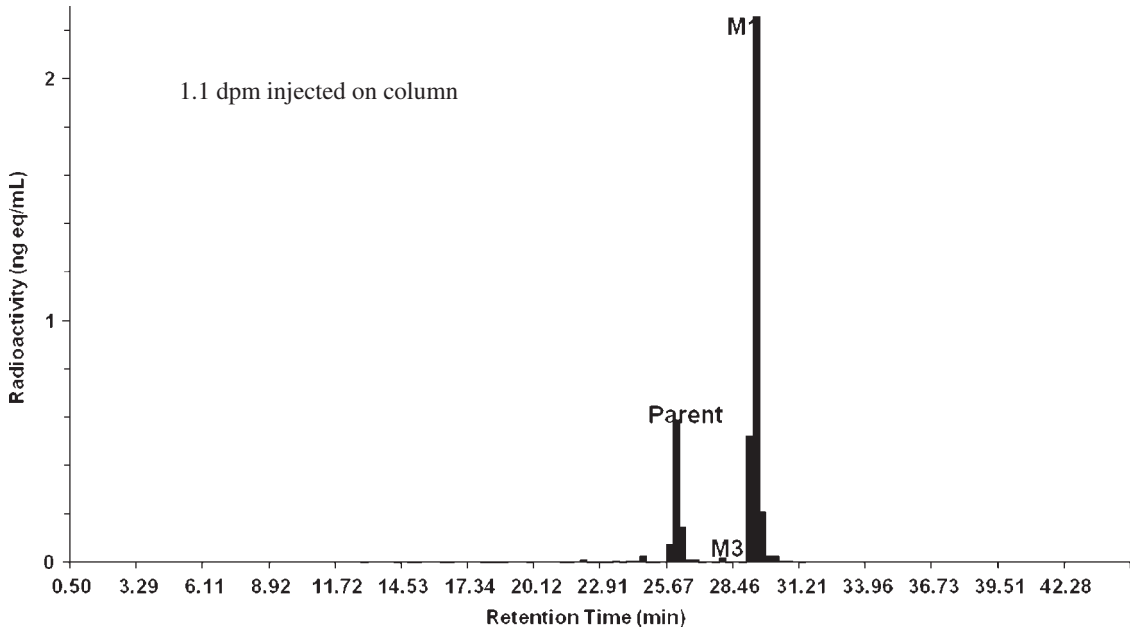

Figure 2. Human plasma AUC pool showing relative proportions of metabolite and parent for a ^{14}C-labelled development drug.

LC/MS analysis is not sufficiently sensitive to replace AMS with this AUC pooling approach as the volume of the pool can be large with later timepoints comprising a much larger percentage of the pool volume than earlier ones. If a new peak of radioactivity is seen in the AUC pool which was not seen either in *in vitro* metabolism studies and/or in preclinical models then semi-preparative HPLC is used to obtain sufficient material for LC/MS and NMR characterisation.

The attraction of this AMS approach is that it enables drug developers to meet the FDA's requirements regarding safety testing of drug metabolites at very little extra cost or loss of time. Indeed finding human specific metabolites late in the drug development process can itself be very costly.

(iii) Absolute bioavailability studies

An understanding of the absolute bioavailability can be very helpful in establishing what factors impact a drug's plasma concentration.[18] Drugs can have low bioavailability through incomplete dissolution, inability to permeate membranes or metabolic instability. Plasma concentrations might be improved through reformulation of the product but not if the poor bioavailability is because of low membrane permeability. The only way to establish precisely which of these factors account for the low bioavailability is to carry out an intravenous administration which guarantees that all the drug reaches the systemic circulation. For drugs that are to be administered by the oral route, drug developers are reluctant to conduct intravenous studies because of the requirement (a) for intravenous toxicology to be performed in two species, one of which is a non-rodent and (b) to produce a suitable intravenous formulation. A novel method has been developed in which a microdose of ^{14}C-labelled drug is administered intravenously concomitantly with an extravascular cold dose of drug. ^{14}C parent drug is analysed by AMS after HPLC separation and cold drug by a suitable analytical method. Absolute bioavailability can then be calculated. The attraction of this approach is that (a) there are no formulation issues since the intravenous dose could be as low as 1 microgram (b) no intravenous toxicology is required since provided oral toxicokinetics have been performed in the appropriate safety test species this provides the necessary cover to permit the intravenous microdose. Figure 3 illustrates data derived from this study design demonstrating that absolute bioavailability studies should become routine much earlier in drug development than historically.

Other applications of AMS in drug development: To date most attention has been focussed on the use of AMS in human ADME studies. This is primarily because ^{14}C-labelled drugs have been used routinely for many years as part of drug development. AMS simply permits similar types of studies to be conducted albeit at much lower radioactive doses.

On the other hand, the exquisite sensitivity of AMS has yet to be fully explored in areas such as biomarker analysis, receptor/ligand interactions, studies on intermediary metabolism, cellular localisation studies and metabolomics. Provided a ^{14}C label can be built into the molecule either endogenously or exogenously then AMS has the capability to follow that molecule as it moves through the body. Whilst not a real time technique, AMS can be used for example with microdialysis where frequent small volume sampling is possible. It can be used to measure drug concentrations in small cell numbers as might be obtained from a biopsy specimen.

Conclusions: It has been demonstrated that AMS is an ultrasensitive technique for measuring ^{14}C and that it can be used routinely in drug development.

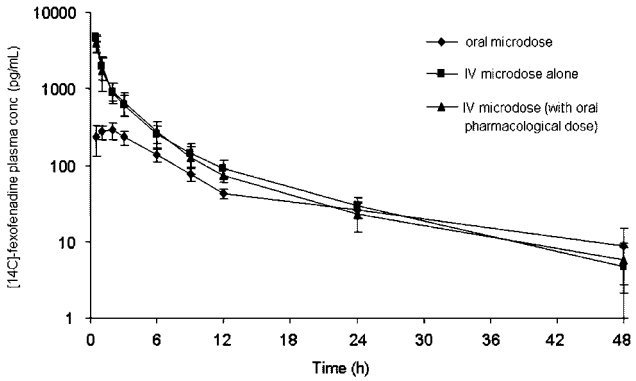

Figure 3. Plasma drug concentrations following administration of ^{14}C-fexofenadine and fexofenadine.

(i) oral microdose −100 μg fexofenadine/7kBq ^{14}C-fexofenadine (ii) intravenous microdose −100 μg fexofenadine/7kBq ^{14}C-fexofenadine (iii) intravenous microdose+oral pharmacological dose–IV 100 μg fexofenadine/7kBq ^{14}C-fexofenadine +120 mg fexofenadine. Plasma ^{14}C-fexofenadine was measured using AMS and unlabelled fexofenadine in (iii) by HPLC with fluorescence detection. (EUMAPP data, manuscript submitted)

Advances in instrumentation, hyphenation with separation techniques and improved sample processing procedures will all come to pass in the years to come thus enabling the use of ^{14}C to continue for many years. Indeed the numbers of studies using ^{14}C can substantially increase using the AMS technology whilst seeing a decrease in the amounts of radioactivity used for research purposes. The consequence will be that the whole infrastructure associated with storage, handling and disposal of ^{14}C will diminish substantially.

References

[1] J. A. DiMasi, R. W. Hansen and H. G. Grabowski, *J Hlth Economics*, **2003**, *22*, 151–185.
[2] US Government Accountability Office, *New Drug Development*, GAO-07-49, GAO **2006**.
[3] www.fiercepharma.com/story/j-j-revenue-sees-first-decline-76-years/2009–01–21.

[4] www.pharmafocus.com/cda/focusH/1,2109,22–0–0-FEB_2009-focus_feature_detail-0-492463,00.html
[5] Challenge and Opportunity on the Critical Path to New Medical Products. US FDA Dept of Hlth Human Services **2004**.
[6] D. A. Katz, B. Murray, A. Bhathena and L. Sahelijo, *Nature Rev Drug Discovery*, **2008**, *7*, 293–305.
[7] A. Roses, *Nature Rev Drug Discovery*, **2008**, *7*, 807–817.
[8] Y. Sugiyama, *Drug Disc Today*, **2005**, *10*, 1577–1579.
[9] www.pelletron.com/ssams14C.pdf
[10] M. Stocker, M. Döbeli, M. Grajcar, M. Suter, H-A. Synal and L. Wacker, *Nucl Inst Methods Phys Res Section B*, **2005**, *240*, 483–489.
[11] J. Barker J and R. C. Garner, *Rapid Commun Mass Spectrom*, **1999**, *13*, 285-293.
[12] M. Gunnarson, K. Stenström, S. Leide-Svegborn, M. Faarinen, C-E. Magnusson, M. Åberg, G. Skog, R. Hellborg and S. Mattson, *Appl Radn Isotopes*, **2003**, *58*, 517–526.
[13] G. Lappin, R. C. Garner, T. Meyers, J. Powell and P. Varley, *J Pharm Biomed Anal*, **2006**, *41*, 1299–1302.
[14] A. Madan, Z. O'Brien, J. Wen, C. O'Brien, R. H. Farber, G. Beaton, P. Crowe, B. Oosterhuis, R. C. Garner, G. Lappin, H. P. Bozigian, *Br J Clin Pharmacol*, **2009**, *67*, 288–298.
[15] G. Lappin, M. Rowland, R. C. Garner, *Expert Opin Drug Metab Pharmacol*, **2006**, *2*, 419–427.
[16] R. C. Garner, *Eur Pharmaceutical Contractor*, **1999**, *11*, 22–28.
[17] Guidance for industry, safety testing of drug metabolites, US FDA, February **2008**.
[18] N. Sarapa, P. H. Hsyu, G. Lappin, R. C. Garner, *J Clin Pharmacol*, **2005**, *45*, 1198–1205.

HIGH SENSITIVITY LABORATORY BASED ^{14}C ANALYSIS FOR DRUG DISCOVERY

ERHAN ILKMEN AND D.E. MURNICK

Department of Physics, Rutgers University, Newark NJ 07102 USA

Abstract: An ultra-sensitive laser-based analytical technique, intracavity optogalvanic spectroscopy (ICOGS) providing extremely high sensitivity for detection of ^{14}C-labeled carbon dioxide has been demonstrated. Obviating the need for scintillation counting and capable of replacing accelerator mass spectrometers (AMS), the technique can quantify zeptomoles of ^{14}C in sub-micromole CO_2 samples. Based on the specificity of laser resonances, coupled with the sensitivity provided by standing waves in an optical cavity, and detection via impedance variations, limits of detection near 10^{-15} $^{14}C/^{12}C$ ratios have been obtained. With the use of a 15 Watt $^{14}CO_2$ laser, a linear calibration with samples from $\approx 10^{-15}$ to $\approx 10^{-11}$ in $^{14}C/^{12}C$ ratios was demonstrated. Calibrations become nonlinear over larger concentration ranges due to laser and ICOGS saturation effects and changes in equilibration time constants. Conditions, however, can be chosen to provide near linear response over different dynamic ranges. Drug discovery applications such as radiolabeling studies with extremely low specific activity, microdosing studies, and individualized sub therapeutic tests of drug metabolism typically involve samples having $^{14}C/^{12}C$ ratios in the approximate range of 1 to 100×10^{-12}. A laboratory instrument for that range will be small (table top), low maintenance and capable of being interfaced to GC or LC inputs.

Keywords: radiocarbon; ^{14}C; drug discovery; microdose; carbon isotopes; optogalvanic spectroscopy

Introduction: Carbon 14 (radiocarbon) is an ideal organic tracer having an extremely low natural abundance in living systems, near 1 ppt, and a long half life, 5730 years, ideal for clinical and laboratory tracer experiments. Accelerator Mass Spectroscopy (AMS), first developed to extend carbon dating to smaller and older samples, has become the standard method for ^{14}C analysis in the field of drug development to obtain pharmacokinetic information on new drug entities using non-therapeutic microdoses of labeled drugs.[1–3] Limitations to wide use of AMS for bioanalytical studies include size, cost and complexity of the analysis system as well as the fact that samples must contain of the order of 0.5 mg total carbon. Now, a new ultrasensitive laser-based analytical technique, intracavity optogalvanic spectroscopy (ICOGS) meets the requirements for ^{14}C quantitation at AMS levels.[4] ICOGS builds on the laser assisted ratio analyzer (LARA) technique[5–7] and is based on the existence of large isotope shifts in molecular spectra, the use of fixed frequency isotopic lasers and sensitive detection via the laser optogalvanic effect (OGE). A $^{14}CO_2$ laser replaces a tandem particle accelerator to provide the required *specificity*. The necessary *sensitivity* is achieved through the optogalvanic effect.[8] If a laser of intensity I, and frequency ν is incident on a cylindrical (length L and radius R) weak electrical discharge, the electrical response, S, of the discharge can be approximately expressed by the product:

$$S = nL_e ffI\sigma K$$

Here, n represents the average molecular density of interacting particles, L_{eff}, the *effective* length of the interaction region, I, the average laser intensity, A, the average area of the laser beam, σ is the laser-species interaction cross section and K is a corresponding optogalvanic proportionality constant that depends on the details of the electrical discharge. Physically, what happens is that the light changes the equilibrium distribution of species, including excited species in the discharge. This affects collision rates, including those between molecules and electrons, leading to a measurable conductivity change, S, of the ionized gas. Optogalvanic spectroscopy for isotopic analysis makes use of the fact that laser resonances in CO_2 are isotope dependent.[9]

Previous success using LARA for breath testing[10–16] and environmental monitoring[17] has led to the development of the technique for the detection of ^{14}C reported here. When the laser operates at a particular transition in $^{14}CO_2$, any resonant change in the

impedance of the discharge system is due to the presence of $^{14}CO_2$ in the discharge. The strongest lasing transitions observed in $^{14}CO_2$ are at 11.8 microns and 11.3 microns, significantly longer in wavelength than lasing transitions of the other 'stable' isotope CO_2 lasers. Any $^{14}CO_2$ molecule in the lower or upper laser level is automatically in resonance (absorption or stimulated emission) with the narrow band laser, providing the sharp specificity required for isotope ratio analysis. The nearest $^{13}CO_2$ and $^{12}CO_2$ lines are separated by more than 500 line widths, leading to non resonant cross sections reduced by approximately 10 orders of magnitude. The nonresonant interaction is further reduced for $^{13}CO_2$ and $^{12}CO_2$ by rotational state Boltzmann population ratios for the two isotopes. In any case, this background effect is pressure dependent and measurable and does not seriously limit the ultimate $^{14}CO_2$ detection limit.

Enhancement of sensitivity in laser absorption experiments often involves increased absorption length (L_{eff}) in optical cavities- most notably cavity ringdown spectroscopy (CRDS)[18] and laser intracavity absorption spectroscopy (ICAS).[19] The new standing wave ICOGS technique is analogous to, but with key differences from, ICAS. The most significant difference from ICAS is that detection is via the OGE rather than optical. The analyte in this case is the same as the lasing species and an OGE exists for stimulated emission and/or absorption.

Experimental: A schematic diagram of the measurement system is shown in Figure 1. The sample cell is placed *inside* a laser cavity (LaserTech Group Inc. Model LTG250, 10 W output with $^{14}CO_2$ fill) thus subjecting it to the full saturated laser power. Also inside the laser cavity is a mechanical chopper used for modulating the beam. The laser output power is used for normalization as well as to monitor the laser's spectral gain profile. The quartz sample cell is 10 cm in length and 22 mm OD, with ZnSe Brewster angle windows. Samples are introduced via the inlet port and trapped in the analysis cell with pressure around 1.1 Torr. In these studies, a radio frequency (rf) glow discharge is utilized because of its stability and low inherent noise.[20] A low power (2 to 5 Watt) rf discharge is ignited and maintained via external copper electrodes. The oscillator power supply circuit also monitors the average rf voltage amplitude across the discharge for the OGE signal. The chopper modulated voltage variation across the cell provides the $^{14}CO_2$ OGE signals.

Time averaged OGE signals were obtained using a National Instruments Data Acquisition System. The virtual instrument designed controlled the chopper, and monitored pressure and laser power.

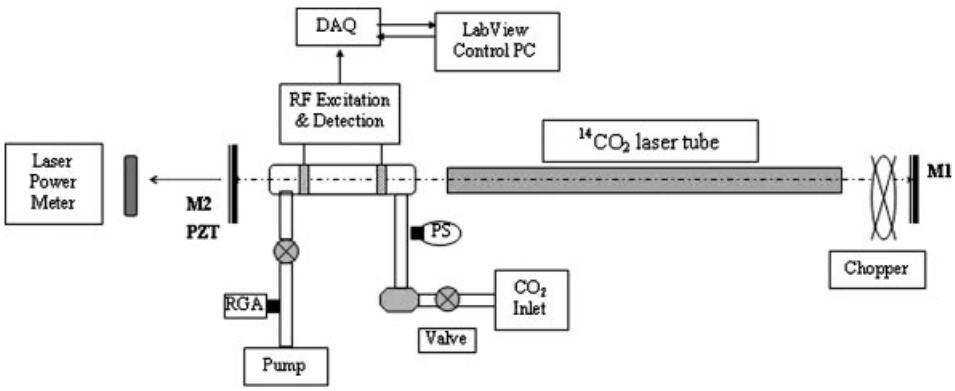

Figure 1. Experimental configuration: The OGE cell inside the cavity has Brewster windows to reduce losses. The chopper inside the laser cavity is for modulating the C14 laser. M1: High reflective mirror & grating, M2: 85% reflective output coupler, PS: Pressure Sensor, FC: Flow Controller, RGA: Residual Gas Analyzer, DAQ: Data Acquisition Board.

Results and Discussion: Figure 2 shows the oge response to a sample of 22 micromoles co_2 with a $^{14}c/^{12}c$ ratio of 1.01×0^{-11}. The figure is a 5 second coherent averaged waveform with the $^{14}co_2$ laser chopped at 63 hz. The observed signal is indicative of a greatly enhanced effective path length over the single pass system due to the intracavity standing wave.

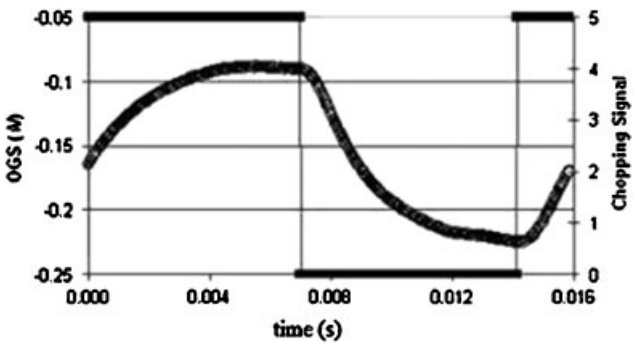

Figure 2. The OGE signal in response to a laser modulated at 63 Hz. The sample is 5% CO_2 in N_2 at 10^{-11} ^{14}C enrichment. The waveform is a 5 second coherent averaged waveform.

The observed mega-enhancement is due to the nature of the optogalvanic effect in the optical cavity. In equation 1 above, I is the circulating internal laser power, around 50 W in our case, and the effective interaction length L_{eff} is given by $c \cdot \Delta t$, where Δt is the time that the laser is on. For a modulation frequency of 63 Hz, Δt is 15.8 msec yielding an effective interaction length of almost 5000 km. This value is close to our observed maximum enhancement of $\sim 10^7$ for the intracavity configuration compared to single

pass. In a multimode ICAS experiment, Δt is given by the spectral saturation time and can be as long as several seconds.[21] In an ICAS experiment what is observed is a change in laser output. The effect on laser output of the few thousand $^{14}CO_2$ molecules in the OGE analysis cell is negligible compared to the 10^{19} active $^{14}CO_2$ molecules in the laser cavity. However, all photon interactions in the intracavity cell contribute to the OGE.

The sensitivity is so great that the natural abundance of ^{14}C in ambient air can easily be detected. The present limit of detection is of order 10^{-15} $^{14}C/C$ ratio, similar to AMS. The optogalvanic proportionality factor for $^{14}CO_2$ in equation 1 is a complicated function of partial pressure for all gas constituents as well as discharge conditions,[22] even changing sign as the system goes from absorption to gain conditions. Also, equation 1 assumes thermal equilibrium, a situation only easily achieved at low concentration and long time. For concentration values greater than the contemporary levels, shorter measurement times and lower pump powers yield larger calibration intervals. For radiocarbon dating of small samples and drug development studies around modern enrichment a calibration region over more than four orders of magnitude has been found using pure CO_2 as the carrier gas, at approximately 1 mbar pressure with a Δt near 60 msec. Figure 3 shows typical calibrations from virtually zero fraction Modern to 12 Modern (1.2×10^{-13} concentration) samples with the OGE signal plotted against AMS results.

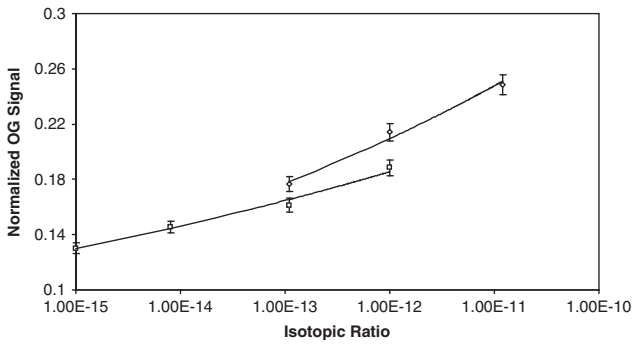

Figure 3. Calibration Curves: Laser power and pressure normalized OGE signals obtained with the ICOGS system plotted against the AMS values. Dynamic range from 10^{-15} to 10^{-12} was obtained with full laser power (lower curve) whereas higher isotope ratios require lower laser power due to laser saturation effects (upper curve).

Due to the fact that the degree of laser saturation is different for higher enrichments, two different calibration intervals are shown for two different laser pump powers. For 1 Modern and below, full laser intensity is utilized whereas for higher concentrations the laser pump power was reduced to decrease the saturation effects. At 100 Modern ratios saturation effects are very pronounced and even lower laser power could be used with a corresponding decrease in dynamic range. A detailed model of the intracavity OGE including laser saturation effects as well as equilibration time constant effects on the OGE parameter K, is currently being studied using ICAS theory[17,19] and OGE theory.[23] As the signal depends on the degree of saturation, the measurement time, the laser power and wavelength as well as buffer gas temperature and pressure, proper conditions must be chosen to balance sensitivity with dynamic range of a measurement.

The system can also be modified to run with continuous flow as shown in Figure 4 where the time dependent response from 1ml CO_2 injected into a gas stream of CO_2 free air as carrier is shown.

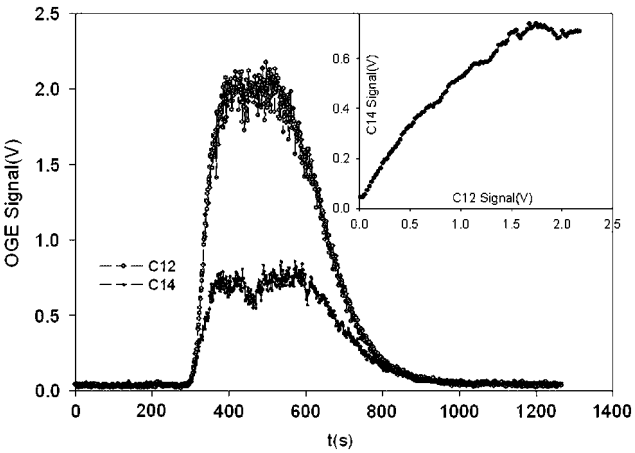

Figure 4. Variation of OGE for ^{12}C (top) and ^{14}C (bottom) as 1 ml is injected into the CO_2 free buffer gas flowing at 10 sccm. As shown in the inset, the signals scale at low concentrations, but the ^{14}C signal saturates at a much lower concentration than the ^{12}C.

Here normalization was achieved with a $^{12}CO_2$ laser beam incident onto the analysis cell through the output coupler of the $^{14}CO_2$ laser. This laser is well separated in wavelength from $^{14}CO_2$ and in resonance with only $^{12}CO_2$ molecules. Time dependent signals for ^{12}C and ^{14}C

are recorded simultaneously as shown in the figure. The saturation effect is obvious when concentration reaches around 1%. Work is in progress to develop hyphenated operation with an LC system via chemical[24] or thermal[25,26] oxidation of the column separations to CO_2.

The sensitivity shown in these and previous AMS experiments will allow more rapid drug development by permitting early safe metabolic testing with microdoses of test compounds.[27] Further, such microdosing studies can be used to customize doses for individual metabolic differences. Though both ^{14}C LARA and AMS aim to quantify ^{14}C in biological samples, there are several significant differences in the technologies. For both techniques, a carbon containing compound is first oxidized to CO_2. The analyte in the LARA technique remains in the form of CO_2, while AMS machines, at present, require an additional step to reduce the CO_2 sample to elemental carbon. There are, however, also significant efforts to enable Bio-AMS machines to run effectively with a gas ion source utilizing CO_2.[28] Normalization to ^{12}C and/or ^{13}C is straightforward with ICOGS for samples of any enrichment, using $^{12}CO_2$ and/or $^{13}CO_2$ lasers as is now done with existing breath and environmental monitoring instruments. Using double ratio techniques with an external reference cell ICOGS is expected to yield precision and accuracy better than 1%. The next two years work is on instrument engineering and technology transfer to the private sector, with the expectation of widespread usage in the pharmaceutical industry within the next five years.

Acknowledgements: This work has been supported by the US NIH (Grant 5R33RR018280), NSF (Grant DBI0456241) and Merck Research Laboratories as well as by the NIH Resource for Biomedical AMS at Lawrence Livermore National Laboratory who have supplied reference samples. Helpful discussions with John Vogel, and Ted Ognibene are appreciated.

References

[1] G. Lappin, R. C. Garner, *Nature Reviews, Drug Discovery* **2003**, *2*, 233.
[2] K. W. Turteltaub, J. S. Vogel, *Curr Pharm Des.* **2000**, *6*, 991.
[3] T. J. Ognibene, G. Bench, J. S. Vogel, G. F. Peaslee, S. Murov *Analytical Chemistry* **2003**, *75*, 2192.
[4] D. Murnick, O. Dogru, E. Ilkmen, *Analytical Chemistry* **2008**, *80*, 4820.
[5] D. E. Murnick, B. J. Peer, *Science*, **1994**, *263*, 945.
[6] D. E. Murnick, M. J. Colgan, D. J. Stonebach, Laser Optogalvanic Isotope Ratio Analysis in Carbon Dioxide, in Synthesis and Applications of Isotopicaly Labeled *Compounds*1997, Editors G. J. Heys, D. G. Melillo, John Wiley and Sons Ltd. **1998**.
[7] D. E. Murnick, J. O. Okil, *Isotopes in Environmental and Health Studies*, **2005** ; *41*, No. 4, 363.
[8] B. Barbieri, N. Beverini, A. Sasso, *Rev Mod Phys*, **1990**, *62*, 603.
[9] C. Freed, Tunable Lasers Handbook, Academic Press, New York, **1995**, pp. 63–165.
[10] B. Braden, C. Gelbmann, C. F. Dietrich, W. F. Caspary, J. Scholmerich, G. Lock, *European Journal of Gastroenterology & Hepatology*. **2001**, *13(7)*, 807.
[11] F. Parente, G. Bianchi-Porro, *European Journal of Gastroenterology & Hepatology*. **2001**, *13*(7), 803.
[12] V. Savarino, F. Landi, P. Dulbecco, C. Ricci, L. Tessieri, R. Biagini, L. Gatta, M. Miglioli, G. Celle, D. Vaira, *Digestive Diseases & Sciences*. **2000**, *45*(11), 2168.
[13] D. R. Cave, V. van Zanten, L. Laine, *Alimentary Pharmacology & Therapeutics*, **1999**, *13*, 747.
[14] R. W. van der Hulst, E. F. Hensen, A. van der Ende, S. P. Kruizinga, A. Homan, G. N. Tytgat, *Nederlands Tijdschrift voor Geneeskunde,* **1999**, *143*, 400.
[15] G. Minoli, A. Prada, R. Schuman, D. Murnick, B. Rigas, *J. Clin. Gastroenterol*; **1998**, *26*, 264.
[16] R. W. M van der Hulst, *Gut*, **1997**, *41*(suppl 1) A72.
[17] J. O. Okil, PhD thesis. Rutgers University Newark NJ **2004**.
[18] Eds. K. W. Busch, M. A. Busch *Cavity-ringdown spectroscopy: an ultratraceabsorption measurement technique* American Chemical Society; ACS symposium series, New York, **1999**, 720.
[19] V. M. Baev, T. Latz, P. E. Toschek, *App. Phys. B* **1999**, *69*(3), 171.
[20] R. D. May, P. H. May, *Rev. Sci. Instruments*, **1986**, *57*, 2242.
[21] H. J. Kimble, *IEEE J of Quantum Electronics*, **1980**, QE-16, 455.
[22] S. Moffatt, A. L. S. Smith, *J .Phys D: Appl. Phys* **1984**, *17*, 59.
[23] A. L. S. Smith, S. Moffatt, S, *J.Phys D: Appl. Phys* **1984**, *17*, 71.
[24] A. L. Sessions, S. P. Sylva, J. M. Hayes, *Anal. Chem*., **2005**, *77*, 6519.
[25] M. Krummen, A. W. Hilkert, D. Juchelka, A. Duhr, H. J. Schlüter, R. Pesch, *Rapid Comm in Mass Spectrometry*, **2004**, *18*, 2260.
[26] R. G. Liberman, S. R. Tannenbaum, B. J. Hughey, R. E. Shefer, R. E. Klinkowstein, C. Prakash, S. P. Harriman, P. L. Skipper. *Anal. Chem.* **2004**, *76*, 328.
[27] G. Lappin, W. Kuhnz, R. Jochemsen, J. Kneer, A. Chaudhary, B. Oosterhuis, W. J. Drijfhout, M. Rowland, R. C. Garner, *Clinical Pharmacology & Therapeutics* **2006**, *80*, 203.
[28] C. B. Ramsey, P. Ditchfield, M. Humm, *Radiocarbon* **2004**, *46* (1), 25.

ULTRA LOW RADIATION BACKGROUND LSC MEASUREMENTS IN A SALT MINE: A FEASIBILITY STUDY

CORINA ANCA SIMION, NICULINA PĂUNESCU, NICOLAE MOCANU, ROMEO CĂLIN, SORIN BERCEA, AND BOGDAN MITRICĂ

Horia Hulubei National Institute for Research and Development in Physics and Nuclear Engineering (IFIN-HH) Magurele-Ilfov, Romania

Abstract: Measurements of long-life radionuclides are developing worldwide by radiometric techniques and mass spectrometry methods too. Both methods offer advantages and disadvantages. In tandem, AMS and LSC techniques provide a powerful working tool. So the techniques provide comparable data for the same types of samples and can support each other in creating a database for a given area, such as the area of Romania. Moreover, ultra low level LSC may be an additional tool for continuous monitoring of environmental conditions in which AMS is current used to measuring the concentration of different contaminants in the air with a high degree of accuracy. To compare the results of applying the above-mentioned techniques, we proposed an analysis of the ideal operational conditions for an ultra low level scintillation spectrometer Quantulus 1220 in two situations: at the surface (IFIN-HH location, where nuclear activities are performed) and underground in a salt mine. The paper presents in detail the scientific and technical aspects as well as predictions on reducing the measurement background with depth, compared with other similar experiments in Europe.

Keywords: ultra low level liquid scintillation counting; underground laboratory; salt mine

Introduction: Measurements of long-life radionuclides such as ^{3}H, ^{14}C, ^{36}Cl, ^{41}Ca, ^{59,63}Ni, ^{89,90}Sr, ^{99}Tc, ^{129}I, ^{135,137}Cs, ^{210}Pb, ^{226,228}Ra, ^{237}Np, ^{241}Am at very low levels, with applications in environmental monitoring, decommissioning of nuclear facilities, radioactive waste storage and tracers in the life sciences are being developed worldwide by radiometric techniques and mass spectrometry methods too.[1]

The specific area of interest of our project is to introduce in Romania an underground LSC technique for environmental monitoring (EM) of tritium, carbon-14 and lead-210 as an initial application which may be comparable with similar investigations in the underground network.

A short characterization of tritium, carbon-14 and lead-210 properties and application fields are presented below in the Tables 1, 2, 3.

Table 1. The sources and main reactions of radionuclides of interest in biological, environmental, and waste samples[1]

Nuclide	Sources	Nuclear reactions for the production of radionuclide
^{3}H	NWT, ONF, RP	^{2}H (n, γ) ^{3}H; ^{3}He (n, p) ^{3}H; ^{6}Li (n, α) ^{3}H
^{14}C	CRR, NWT, ONF, RP	^{14}N (n, p) ^{14}C; ^{13}C (n, γ) ^{14}C; ^{17}O (n, α) ^{14}C
^{210}Pb	Natural decay series	U-238

NWT: nuclear weapon testing; ONF: operation of nuclear facilities; CRR: cosmic ray reaction; RP: reprocessing plants

Table 2. Radionuclides of interest in biological, environmental, waste samples and their applications[1]

Nuclides	Atom mass	Half-life	Decay mode	Specific activity (Bqg−1)	Application fields
^{3}H	3.0161	12.3 y	$\beta-$	3.57×10^{14}	**EM**, DN, MT
^{14}C	14.0032	5730 y	$\beta-$	1.65×10^{11}	Dating, DN, **EM**
^{210}Pb	209.9842	22.3 y	$\beta-$	2.83×10^{12}	Dating, **EM**

EM: environmental monitoring; DN: decommissioning of nuclear facilities; MT: medical tracer

Table 3. Energies of β particles of the radionuclides and the detection limits of beta liquid scintillation counting (LSC)[1]

Radionuclides	Decay	Emax (keV) (abundance)	Ld of LSC (g)
^{3}H	$\beta-$	18.6	$\mathbf{2.50 \times 10^{-17}}$
^{14}C	$\beta-$	156.5	$\mathbf{7.41 \times 10^{-14}}$
^{210}Pb	$\beta-$	17.0 (84%), 63.5 (16%)	$\mathbf{8.40 \times 10^{-15}}$

The limit of detection (LoD) of accelerator mass spectrometry (AMS) is well below 10^{-10} g (usually 10^{-15} g).[1–3] Due to the high price, there are less than 100 AMS facilities worldwide, in which most of them are mainly used for the routine analysis of C-14 for dating purposes. Although many AMS's have the ability to analyze of many long-lived radionuclides, most of these AMS only determine very few of these radionuclides routinely. The main drawback with AMS is that it is only applicable to those elements that form negative ions during the sputtering process, also the lack of flexibility in changing from one element of interest to another.[1] Therefore for a greater accesibility we must lower the LoD in LSC, especially for carbon-14 measurements using: an ultra low level liquid scintillation analyzer such as the Quantulus 1220 (Wallac-Turku-Finland); an underground laboratory facility such as Gran Sasso National Laboratory (LNGS, Italy); both ultra low level analyzer and an underground laboratory. But, do we really need both or the Quantulus 1220 and the underground laboratory to reach the AMS LoD? The LoD in LSC depends on the background radioactivity. Background is introduced by inherent radioactivity of the phototubes, sample containers, cosmic particles and their secondari radiolysis and by environmental gamma radiation. The most important factor for the low level counting procedures is the stability of the counter background. Thus, elevated, stable background is far better than low variable background. To achieve stability, one must have a stable instruments,

environments and the sample.[4] We can't influence the inherent radioactivity of the phototubes, but we can bring down the contribution of sample containers, vials, cosmic particles and environmental background in an underground laboratory.[5–10]

The effective background count rate in the tritium window in the underground laboratory (LNGS, Italy) is two times lower than that in the above ground laboratory due to better shielding of the cosmic rays.[7] The data indicates a background reduction of approximately 65% between the surface and underground laboratories, with no differences in the efficiency for carbon-14.[8]

There is an advantage of having the laboratory built underground where cosmic radiation is attenuated by masses above the LSC. It is not, however, a necessary requirement. Risk of elevated radon concentrations need to be considered in underground installations. Therefore, the most important factor in the determination of Quantulus background is the gamma photon flux from the counting environment as seen in the Table 4.[4]

Table 4. Factors influencing background

Factors influencing background	Gran Sasso National Laboratory (LNGS)[1]	Solotvina Underground Laboratory (SUL)[1]	Unirea salt Mine Romania[11,12]
Depth	1400 m (3800 m.w.e.)	430 m	208 m (~560 m.w.e.)
Gamma photon flux	Approx. 100 times higher than in a salt mine	10–100 times lower *than in other underground laboratories*	80–90 times lower than the surface
Muon flux	1.1 μm^{-2} h^{-1}	62 μm^{-2} h^{-1}	>62 μm^{-2} h^{-1} (expected value)
Neutron flux	$1.08 \cdot 10^{-6}$ n cm^{-2} s^{-1} (0–0.05 eV) $1.84 \cdot 10^{-6}$ n cm^{-2} s^{-1} (0.05 eV–1 keV) $0.54 \cdot 10^{-6}$ n cm^{-2} s^{-1} (1 keV–2.5 MeV) $0.32 \cdot 10^{-6}$ n cm^{-2} s^{-1} (>2.5 MeV)	$< 2.7 \cdot 10^{-6}$ n cm^{-2} s^{-1} (integrated)	$> 2.7 \cdot 10^{-6}$ n cm^{-2} s^{-1} (integrated); expected value
Radon	80–100 Bq/m^3	Low content	< 10 Bq/m^3
K-40	160 ppm in rock	Very low content	Non-detectable in salt
U-238	6.8 ppm in rock (Hall A) 0.42 ppm in rock (Hall B) 0.66 ppm in rock (Hall C) 1.05 ppm concrete (All Halls)	Very low content	0.92 ± 0.3 in salt
Th-232	2.167 ppm in rock (Hall A) 0.062 ppm in rock (Hall B) 0.066 ppm in rock (Hall C) 0.656 ppm concrete (All Halls)	Very low content	Non-detectable in salt

Experimental: A comparison between two surface laboratories (IFIN-HH) and another underground laboratory facility (Unirea salt mine) is presented in the Table 5.

Results and Discussion: Previous radioactivity measurements for Uranium, ^{40}K and ^{222}Rn in the deposit of a salt mine located at about 100 km distance from IFIN-HH showed lower activities than those found in some underground laboratories in Europe. According to the literature, the mentioned radionuclides are considered as main contaminants inside the granitic mines. They are known to influence negatively LSC measurements. Gamma radiation background found inside the salt mine (another factor influencing negatively the quality of LSC measurement results) was lower too, with three orders of magnitude less than that measured outside the mine. The only shortcoming of the location in the salt mine is the mean depth (~600 m.w.e.), this causes a less reduction of the cosmic ray contribution (muon and neutron fluxes) influencing the LSC measurements. For proper evaluation of the cosmic ray contribution to the spectrum it is necessary to establish a parallel monitoring of muonic flux (at energies in GeV range) by means of a radioantenna, as in the case of one our projects performed in an underground location. The major disadvantages for the Unirea salt Mine seems to be: the depth, the muon flux, the neutron flux and the corrosion factor.[11–13]

Other sources of variable background values are; the temperature, pressure and humidity changes in the counting room. Air conditioning system is recommended. A Faraday cage is recommended to lesser electromagnetic interference from noisy power lines. The counting room should not receipt direct sunlight. Background samples must be prepared and stored in the counting room. Gamma sources stored outside the counting room; pulsed accelerator in a distance; dust or cigarette smoke should be allowed in the counting room.[4]

The ideal location for the underground laboratory seems to be Unirea salt mine, but there are other factors influencing the final decision: the distance between the institute and the underground laboratory (supplementary expenses); other plans concerning Unirea salt mine development; the stability of the salt mine; funds and future projects.

Conclusion: The Unirea salt mine may be the ideal location for developing of an ultra low background counting room for LSC technique by IFIN-HH and it has with some advantages and disadvantages. A good alternative is a surface location at IFIN-HH Group 2.

Table 5. The main parameters of three locations for the ultra low level laboratory

Factors influencing background	IFIN-HH Group 1	IFIN-HH Group 2	Unirea salt mine
Muon flux (GeV)	$\sim 3060\ \mu/m^2\,h$	$\sim 3060\ \mu/m^2\,h$	Estimated value $\geq 62\ \mu/m^2\,h$; to be correctly determined in a new project (as m.w.e.)
Neutron flux (integrated value)	≤ 10 nSv/h	≤ 10 nSv/h	Estimated value: $> 2.7\ 10^{-6}\ n/cm^2\,s$; to be correctly determined in a new project
Rn-222 (indoor)	69.2 Bq/m^3	24.5 Bq/m^3	< 10 Bq/m^3
K-40	11.3 ppm	11.3 ppm	1.54 ± 0.30 ppm in sediment, not detectable in salt rock (the sediment represents $\sim 1.16\%$ of the total mass rock)
U-238 Th-232(concrete/bricks)	U-238: 2.3 ppm/ 8.2 ppm Th-232:2.1 ppm/ 10.8 ppm;	U-238: 2.3 ppm/ 8.2 ppm; Th-232: 2.1 ppm/10.8 ppm	U-238: 5.15 ± 0.51 ppm in sediment, not detectable in salt rock Th-232: 5.56 ± 0.07 ppm in sediment, not detectable in salt rock (the sediment represents $\sim 1.16\%$ of the total mass rock)
Tritium as HTO (indoor)	40.2 ± 6 Bq/L	< 5 Bq/L	< 5 Bq/L
Carbon-14 (indoor)	Not determined	Not determined	Not determined
Gamma flux radiation	$\leq 0.2\ \mu$Gy/h	45.63 nGy/h	1.17 nGy/h
Mobil phone antenna	Far	Near	Very close
Noisy power lines	Detected	Detected	Non-detected
Pulsed accelerator	Ciclotron, Tandem, AMS (in the future)	Non-existent	Non-existent
Pressure	Variable	Variable	Constant
Temperature	Variable	Variable	Constant: 15–17°C
Humidity	Variable	Variable	Constant: 65−70%
Light	Sun light	Sun light	Incandescent lighting & total dark ~ 18 h/24 h
Corrosion factor	Non-detected	Non-detected	Greater than the surface with an order of magnitude

This location, near the dendrological park of the institute, is an ideal place for preparing samples, because the experiments on real material have shown that the problems in extending the limit of detection of carbon-14 historically have much more to do with benzene synthesis and contaminants introduced through lithium, surface reaction catalysts and impurities than the counter background level.[15]

The final decision on the placement of the ultra low level laboratory strongly depends on the measured muon and neutron flux and the special design of counting room. We must seriously take into account the reduction of corrosion factors, longterm stability of the old salt mine and some official decisions and funds.

Acknowledgements: Authors would like to thank the National Authority for Scientific Research–National Centre for Program Management Romania for funding the project No. 51–053/2007 also the International Atomic Energy Agency for sponsorising the presentation of this conributed paper at the Tenth International Symposium on Isotopes and Isotopically Labelled Compounds, Chicago 2009, and the Canberra-Packard representative in Romania.

References

[1] X. Hou, Per Roos, Anal. Chim. Acta, **2008**, *608*, 105–139.
[2] Ch. B. Ramsey, Th. Higham, Ph. Leach, Radiocarbon, **2004**, *46(1)*, 17–24.
[3] P. Steier, F. Dellinger, W. Kutschera, A. Priller, W. Rom, E. M. Wild, Radiocarbon, **2004**, *46(1)*, 5–16.
[4] PerkinElmer, 'Low background counting requirements', July **2006**.
[5] U. Schotterer, H. Oeschger, Radiocarbon, **1980**, *22(2)*, 505–511.
[6] Sh. Bowman, Radiocarbon, **1989**, *31(3)*, 393–398.
[7] I. Schäfer, D. Herbert, U. Zeiske, Appl. Rad. and Isotopes, **2000**, *53*, 309–315.
[8] W. Plastino, L. Kaihola, P. Bartolomei, F. Bella, Radiocarbon, **2001**, *43(2A)*, 157–161.
[9] Transnational Access to Research Infrastructures. Project number: P08/02. Final scientific report. Project Title: Ultra-low level detection of the tritium groundwater samples for liquid scintillation spectrometry at underground laboratory Gran Sasso LNGS Access period: November 2002-April 2003.
[10] W. Plastino, Radiocarbon, **2004**, *46(1)*, 97–104.
[11] R. Margineanu, C. Simion, S. Bercea, D. Gheorghiu, M. Matei, *'Underground laboratory for measurement in ultra-low radiation background in Romania'*, CELLAR meeting, Gran Sasso, 29–30 June, **2006**.
[12] R. Margineanu, C. Simion, S. Bercea, O. G. Duliu, D. Gheorghiu, A. Stochioiu, M. Matei, Appl. Rad. and Isotopes, **2008**, 66, 1501–1506.
[13] L. Miramonti, *'European Underground Laboratories: An overview'*, LRT 2004-Topical Workshop in Low Radioactivity Techniques, Sudbury, Canada, December 12–14, **2004**.

[14] W. Plastino, L. Kaihola, P. Bartolomei, F. Bella, Radiocarbon, **2001**, *43(2A)*, 157–161.
[15] Radnell and Muller, 1980; Lowe, 1989; McCormac et al., 1993.

A SYSTEM FOR THE RADIOCHEMICAL PURIFICATION OF MICROFLUIDICS-GENERATED COMPOUND

JIANZHONG ZHANG, ARKADIJ ELIZAROV, REZA MIRAGHAIE, ED BALL, AND HARTMUTH KOLB

Siemens Molecular Imaging, 6100 Bristol Parkway, Culver City, CA 90230, USA

Abstract: An automated purification system has been developed for microfluidics-generated compounds, such as 3-Deoxy-3-[^{18}F]fluorothymidine ([^{18}F]FLT), using a USB data acquisition device and LabVIEW software. The purification is based on HPLC separation and radioactivity/UV absorbance detection. The linear range of radioactivity measurement is from 1 μCi to 200 mCi with a detection limit of 0.15 μCi. However, the system can measure radioactivity as high as 2 Ci. Each purification process allows either automatic or manual collection of multiple fractions, one of which can be further reformulated for *in vivo* biomarker studies.

Keywords: radiosynthesis; purification; automation; detection; microfluidics

Introduction: Microfluidics has advantages, including reagent conservation, reaction speed and product yield, in producing short-lived radiochemical compounds for positron emission tomography (PET) imaging[1–4]. Based on quality requirements, these compounds have to be purified before being injected in *in vivo* applications. Since most positron emitters, such as ^{18}F ($t_{1/2}$ = 109.8 min) and ^{11}C ($t_{1/2}$ = 20.4 min), are short-lived, both radiochemical synthesis and subsequent purification have to be as fast and efficient as possible. In this article we describe a purification system that provides for the isolation of microfluidics-generated ^{18}F-labeled compounds. [^{18}F]FLT, for example, can be purified within 10 minutes after crude reaction mixture is transferred from a microfluidic synthesizer to the purification system.

Material and Method: Radiochemical synthesis of [^{18}F]FLT

[^{18}F]Fluoride was generated through the 11 MeV proton bombardment of [^{18}O]H_2O via ^{18}O(p,n)^{18}F nuclear reaction. [^{18}F]FLT was synthesized from a non-radioactive precursor through fluorination and hydrolysis. Briefly, the precursor reacted with concentrated [^{18}F]fluoride in acetonitrile at 200°C in the presence of Kryptofix 2.2.2, and then was hydrolyzed to form [^{18}F]FLT with hydrochloric acid at 120°C.

Chemicals

The [^{18}F]FLT precursor, (t-Bu-((2R,4R,5R)-5-((t-butoxycarbonyloxy)methyl)-4-(nitrophenylsulfonyloxy) tetrahydrofuran-2-yl)-5-methyl-2,6-dioxo-2,3-dihydro-pyrimidine-1-(6H)-carboxylate), was obtained from Syntagon Baltic (Södertälje, Sweden). Kryptofix 2.2.2 (4,7,13,16,21,24-hexaoxa-1,10-diazabicyclo[8,8,8]hexacosane) was purchased from Aldrich (St. Louis, MO). HPLC water and hydrochloric acid were purchased from Fisher Scientific (FairLawn, NJ). Dehydrated alcohol was purchased from Spectrum (Gardena, CA). Acetonitrile was obtained from Acros Organics (Morris Plains, NJ).

Instruments

A schematic of the instrument is shown in Figure 1.

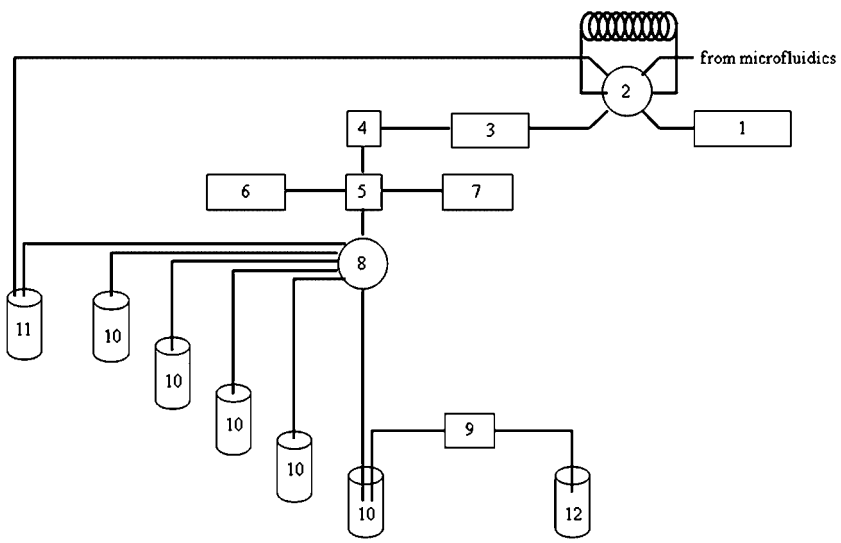

Figure 1. A schematic of the purification system. 1. HPLC pump; 2. loop valve; 3. monolithic C18 column; 4. radioactivity detector; 5. UV detection cell; 6. UV light source; 7. UV detector; 8. 6-position distribution valve; 9. reconstitution cartridge; 10. fraction collecting vials; 11. waste container; 12. final product vial.

A K501 HPLC pump (Knauer, Berlin, Germany) was used to pump solvent through a 10 mm × 100 mm Onyx semi-preparative C18 column (Phenomenex, Torrance, CA) for purification. A valve was placed in front of the pump to select solvent (not shown). A 2-position loop valve (Rheodyne, Rohnert Park, CA) was used for sample loading from the microfluidic synthesizer into the purification system and a 6-position distribution valve (Rheodyne, Rohnert Park, CA) was used for waste and for multiple fraction collection. The system had two detection channels: radioactivity and UV absorbance. For [^{18}F]FLT, the wavelength for UV absorbance measurement was set at 265 nm. A L10290 UV-VIS light source (Hamamatsu, Bridgewater, NJ) and a USB-4000 spectrometer (Ocean Optics, Dunedin, FL), both equipped with fiber optics, were used for UV absorbance measurement, while a model 105S-1 CsI(Tl)-photodiode based radioactivity detector (Carroll & Ramsey Associates, Berkeley, CA) was used for radioactivity detection. A USB-6009 data acquisition device (National Instruments, Austin, Texas) was used for data acquisition and instrument control. Data acquisition and control software was written with LabVIEW 8.2 (National Instruments, Austin, Texas). Radioactive thin layer chromatography (TLC) was read out with an AR-2000 radio-TLC imaging scanner (Bioscan, Washington, DC).

Other than the USB-4000 spectrometer, which is used for UV absorbance measurement at the given wavelength, the rest of the purification system is build around an economical NI USB-6009 data acquisition device. This device provides 1) analog input, which is used for measurement of radioactivity, temperature and pressure; 2) analog output, which is used to control HPLC flow rate; 3) digital input, which is used to indicate valve position; and 4) digital output, which is used to control valve operation. In addition, the device has a 32-bit counter, which provides a more sensitive approach for radioactivity measurement than with analog input–sub-μCi can be detected with a CsI(Tl)-photodiode detector.

The purification system features two detection channels: a UV detection channel and a radioactivity detection channel, with radioactivity detector being placed directly on top of the UV flow cell. The design enables simultaneous signal measurement from both channels and ensures reliable purification information.

The porous structure of the monolithic C18 column allows low back-pressure and high speed operation.[5] It is possible to directly pressure transfer the product from microfluidic synthesizer onto the column for HPLC purification. In practice, we choose to use an injection valve, which has a 1 ml sample loop, for more reliable sample transfer. As shown in Figure 3c, the whole [^{18}F]FLT separation process takes 20 minutes, but the [^{18}F]FLT fraction can be obtained in less than 10 minutes, including a 5 minute water wash at the beginning.

Results: *Radioactivity measurement*

The radioactivity response of the detection system is characterized by injecting a series of 100 μl [^{18}F]fluoride solutions into the purification system. The solvent used is HPLC- grade water, pumping through the monolithic semi-preparative column at a rate of 4 ml/min. The average peak area ($n = 3$, decay corrected) of the [^{18}F]fluoride is plotted against the [^{18}F] fluoride concentration to generate a calibration curve (Figure 2).

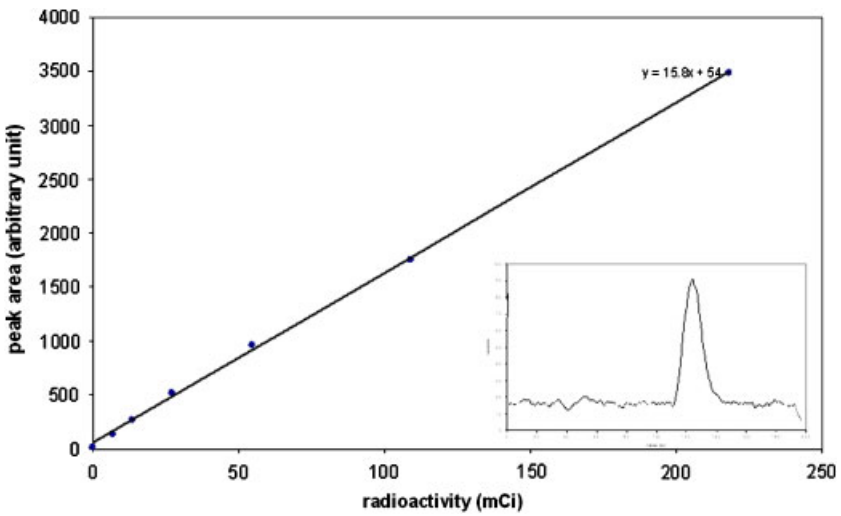

Figure 2. Calibration curve of the HPLC radioactivity measurement. The insert is a peak corresponding to 6.8 μCi of [^{18}F]fluoride loaded onto the monolithic C18 column.

The linear range of the radioactivity measurement is from 1 μCi to 200 mCi with the detection limit of 0.15 μCi. The peak in the insert corresponds to an injection of 6.8 μCi [^{18}F]fluoride. It should be noted that in our routine purification the detection system can measure radioactivity as high as 2 Ci, which is beyond the linear range.

Chromatographic purification

Through fluorination and deprotection, [^{18}F]fluoride reacts with the precursor to form [^{18}F]FLT with certain efficiency. Usually, the precursor is in large access for better use of [^{18}F]fluoride. TLC of a typical microfluidic synthesis shows a radioactivity profile: [^{18}F]fluoride (33%), [^{18}F]FLT (62%) and unhydrolyzed intermediate (5%).

Journal of
Labelled Compounds and
Radiopharmaceuticals

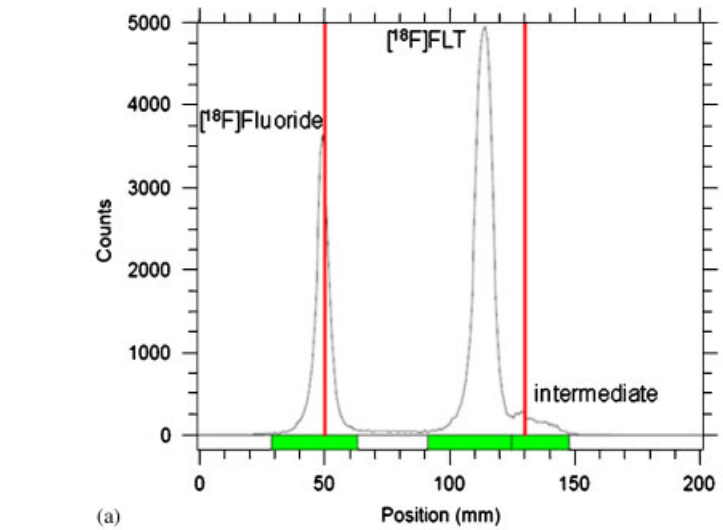

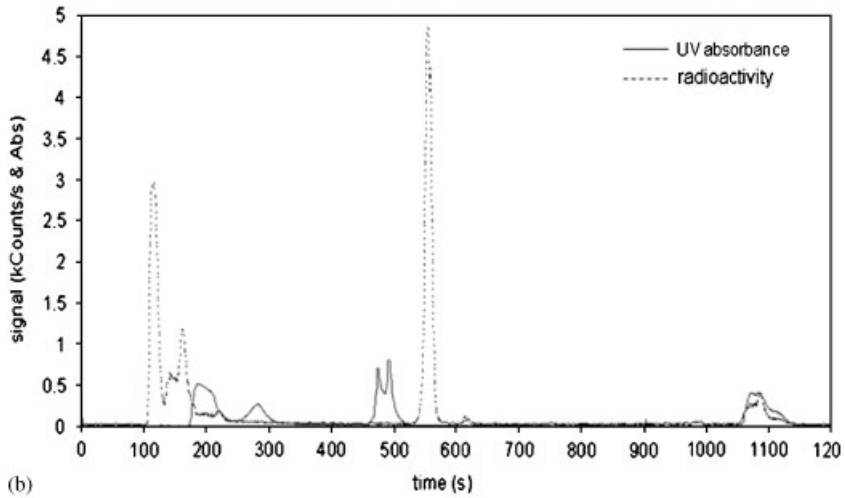

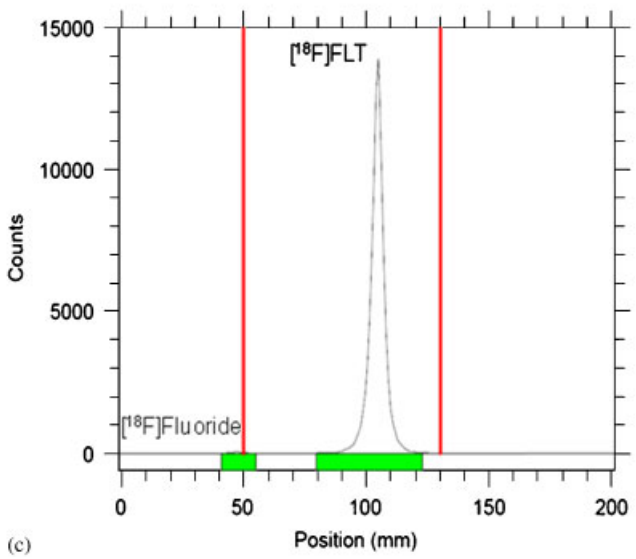

Figure 3. (a) A TLC chromatogram showing the composition of the microfluidics-generated product. The raw product contains [^{18}F]Fluoride (33%), [^{18}F]FLT (62%) and unhydrolyzed intermediate (5%); (b) A HPLC chromatogram showing UV absorbance and radioactivity traces for the separation of the microfluidics-generated [^{18}F]FLT. Three solvents are used for the separation water (0–300 s); 8% ethanol (301–900 s); actonitrile (901–1200 s) The [^{18}F]FLT pak is at 560 s; and (c) A TLC chromatogram showing the composition of the purified, microfluidics-generated product. The purified product contains [^{18}F]fluoride (0.6%) and [^{18}F]FLT (99.4%).

The HPLC Chromatogram clearly shows three major regions of radioactivity.

We choose to elute [^{18}F]fluoride (and hydrophilic byproduct) with HPLC-grade water (0 to 300 s), [^{18}F]FLT with 8% ethanol (301 to 900 s) and unhydrolyzed intermediate with 100% acetonitrile (901 to 1200 s). The [^{18}F]FLT fraction can be collected either automatically or manually. A post purification TLC indicates that only very small amount (0.6%) of [^{18}F]fluoride is in the purified [^{18}F]FLT.

Discussion: Bourgeois *et al*. studied the HPLC purification of [^{18}F]FLT [6]. Our approach, however, is somewhat similar to that reported by Grierson and Shields [7], who found that the C18 HPLC column has the ability to pre-concentrate FLT from a large injected volume of water. We believe that starting purification with a few minute water wash is worthwhile. First, it washes out [^{18}F]fluoride during the early stage of purification, making the background low and flat before the elution of [^{18}F]FLT; second, the peak of [^{18}F]FLT becomes sharper and more symmetrical. As a result, a high quality [^{18}F]FLT fraction is obtained (see Figure 3c for the TLC result).

In [^{18}F]FLT (or other radioactive compound) purification, the baseline of the chromatogram varies, depending on the amount of radioactivity transferred from microfluidic synthesizer. Therefore, to setup a threshold at the beginning of the purification is not practical. Instead, we choose to setup a time, at which the [^{18}F]FLT is about to come out. The time in turn dynamically sets up a threshold for [^{18}F]FLT fraction collection. Considering noise and fluctuation of the background, a tolerance is given on top of the threshold level. Another option might be to use slope, or derivative, of the chromatographic signal to automatically determine the start and end of a fraction. A manual fraction control is provided in the purification program, which overrides the automated function. After a fraction is collected, the distribution valve moves to next vial, ready for next fraction.

The first fraction, which usually contains the desired radioactive compound, has the option for further solvent reformulation with the use of a solid phase extraction cartridge, whenever its specific concentration (defined as radioactivity/mass ratio) is not high enough or the solvent in the fraction is not compatible with *in vivo* application. The reformulation process is fully automatic, which includes the processes of sample dilution, sample trapping, cartridge rinsing and sample elution.

Conclusion: We have described an automated and microfluidics-compatible purification system. The system allows us to directly transfer product from microfluidic device to purification column, simultaneously measure UV and radioactivity signals and rapidly generate high quality radioactive products.

References

[1] A. M. Elizarov, *Lab on a Chip,* **2009**, *9*, 1326–1333.
[2] L. Cai, S. Lu and V. W. Pike, *Eur. J. Org. Chem.,* **2008**, *17*, 2853–2873.
[3] C. C. Lee, G. D. Sui, A. Elizarov, C. Y. J. Shu, Y. S. Shin, A. N. Dooley, J. Huang, A. Daridon, P. Wyatt, D. Stout, H. C. Kolb, O. N. Witte, N. Satyamurthy, J. R. Heath, M. E. Phelps, S. R. Quake and H. R. Tseng, *Science*, **2005**, *310*, 1793–1796.
[4] A. M. Elizarov, R. M. van Dam, Y. S. Shin, H. C. Kolb, J. R. Heath, H. C. Padgett, D. Stout, J. Shu, J. Huang, A. Daridon, *J Nucl Med.,* **2010**, in press.
[5] F. Svec, *Recent Developments in LC Column Technology*, **2003**, *6*, 2–6.
[6] M. Bourgeois, M. Mougin-Degraef, F. Leost, M. Cherel, J. Gestin, D. L. Bars, J. Barbet and A. Faivre-Chauvet, *J. Pharm. Biomed. Anal.,* **2007**, *45*, 154–157.
[7] J. R. Grierson and A. F. Shields, *Nucl. Med. Biol.,* **2000**, *27*, 143–156.

